

Non-equilibrium structure and relaxation in active microemulsions

Rakesh Chatterjee^{1,2}, Hui-Shun Kuan^{1,2,3}, Frank Jülicher^{4,5,6}, and Vasily Zaburdaev^{1,2}
¹ *Department of Biology, Friedrich-Alexander-Universität Erlangen-Nürnberg, Erlangen, Germany*
² *Max-Planck-Zentrum für Physik und Medizin, Erlangen, Germany*
³ *TSMC, Hsinchu Science Park, Hsinchu, Taiwan*
⁴ *Max Planck Institute for the Physics of Complex Systems, Dresden, Germany*
⁵ *Center for Systems Biology Dresden, Dresden, Germany*
⁶ *Cluster of Excellence Physics of Life, TU Dresden, Dresden, Germany*

Microphase separation is common in active biological systems as exemplified by the separation of RNA and DNA-rich phases in the cell nucleus driven by the transcriptional activity of polymerase enzymes acting similarly to amphiphiles in a microemulsion. Here we propose an analytically tractable model of an active microemulsion to investigate how the activity affects its structure and relaxation dynamics. Continuum theory derived from a lattice model exhibits two distinct regimes of the relaxation dynamics and is linked to the broken detailed balance due to intermittent activity of the amphiphiles.

A broad range of complex biological phenomena [1–4] as well as man-made systems of active matter [5–7] motivated the development of theoretical concepts borrowed or generalized from equilibrium statistical mechanics. In some regimes, equilibrium theory remains valid even in an intrinsically out of equilibrium context of a living cell [8], sometimes it is applied phenomenologically [9, 10], and sometimes truly non-equilibrium models are put forward [11]. Further examples include the hydrodynamics of flocks and active self-propelled particles [12, 13], and the active gel theory of the cell skeleton and beyond [14]. Currently, a broad range of biological applications is found in the theory of liquid-liquid phase separation [15, 16] and specifically in the concept of active microemulsion [17] that describes the organization of complex multi-phase systems. However, theoretical understanding of nonequilibrium effects in microemulsion systems is still very limited. Here, motivated by a biological process of chromatin organisation by transcription, we formulate an active microemulsion model and investigate the effects of activity on its structure and relaxation dynamics.

Transcriptionally active nuclei exhibit the phenomenon of microphase separation into DNA-rich and RNA-rich domains [18]. It has been suggested that polymerase molecules engaged in the process of transcription can have an effect similar to amphiphiles in a prototypical oil-and-water emulsion [19, 20]. The process of transcription itself is active as manifested by its intermittent dynamics and by the production of the RNA-component. While it is well understood how in passive systems the presence of amphiphiles determines the process of microphase separation (via several theoretical and numerical approaches [21–30]), how the activity of amphiphiles could change the microemulsion structure and relaxation dynamics has not yet been explored.

Starting with a generalization of the Gompper-Schick lattice model of a microemulsion [31] we show that an amphiphile that intermittently switches from an active to an

inactive state can change the structure of the microemulsion. We then coarse-grain the lattice model to develop a continuum version of the theory and find a two-regime relaxation dynamics of active microemulsions. The two regimes of relaxation can be attributed to the fast amphiphile turnover and slower diffusion of phases respectively. Finally, we can link the local entropy production at the amphiphile-rich interface to the nonequilibrium amphiphile turnover dynamics. Our theory will help to better understand the non-equilibrium patterning processes in active multi-phase systems.

Biological motivation and model.- To investigate the role of amphiphilic activity, we establish a phenomenological model, which qualitatively captures the experimental observations on microphase separation in the cell nucleus [18]. DNA and mRNA, produced during transcription, are the two phase-separating components. Polymerase molecules that attach to DNA and perform transcription by producing mRNA-transcripts thereby connect the two segregating phases and therefore act as amphiphiles. This configuration with three basic components is similar to the ternary oil-water-amphiphile system, which exhibits two- and three-phase coexistence [29]. However, unlike in the classical example, amphiphile-like activity of polymerases is intermittent [32–34]: polymerases bind to DNA and engage in transcription, moving persistently along the DNA strand but then unbind from DNA when reaching the end of the transcribed gene. We thus aim to model this intermittent amphiphile dynamics by introducing the switching of the amphiphile between “active” state when it reduces the system’s energy at the interface between the two phases, and “inactive” when it does not.

Lattice model of microemulsion.- We first start with the lattice-based implementation of the active microemulsion model building upon the work of Gompper and Schick [31, 35, 36]. A square lattice of size $L \times L$ contains two phase-separating components A and B , while Ω acts as an amphiphile, with an individual element of each component occupying a single lattice site (see Fig.1). We use

the size of the single lattice site as the length scale and set it to be equal to 1 for the rest of the manuscript. A and B exhibit self-affinity with parameters J_{AA} and J_{BB} respectively and repel each other as parameterized by J_{AB} . Amphiphiles Ω in the “active” state reduce the system’s energy by the value J_{Ω} if placed on a line flanked by A and B species (see Fig.1). Inactive amphiphiles do not contribute to the energy of the system. Here we introduce intermittent activity by switching the functional amphiphiles to the inactive state with rate k_{off} and back to the active state with rate k_{on} .

The Hamiltonian of a four-component system (two phases and two states of the amphiphile) is described in terms of occupancy operators $\eta_i^{A,B,\Omega,\Omega_I}$, which are equal to unity if a site i is occupied by the respective component A, B, Ω, Ω_I and zero otherwise, and interaction strengths J_{ij} for two phases $i, j = \{A, B\}$ and amphiphile-mediated interaction J_{Ω} :

$$\mathcal{H} = -\frac{1}{2} \sum_{\langle ij \rangle} \left(J_{AA} \eta_i^A \eta_j^A + J_{BB} \eta_i^B \eta_j^B + J_{AB} (\eta_i^A \eta_j^B + \eta_i^B \eta_j^A) \right) - \frac{J_{\Omega}}{2} \sum_{\langle ijk \rangle} \left(\eta_i^A \eta_j^{\Omega} \eta_k^B + \eta_i^B \eta_j^{\Omega} \eta_k^A - \eta_i^A \eta_j^{\Omega} \eta_k^A - \eta_i^B \eta_j^{\Omega} \eta_k^B \right) \quad (1)$$

The first term is the sum over same and distinct component pair interactions. The second term represents the contribution of amphiphile-mediated interaction where amphiphiles reduce the system energy when placed between A and B and increase the system energy when flanked by similar lattice species. There is an intermittent dynamics of amphiphile activity $\eta_i^{\Omega} \xrightarrow{k_{\text{off}}} \eta_i^{\Omega_I}$, $\eta_i^{\Omega_I} \xrightarrow{k_{\text{on}}} \eta_i^{\Omega}$, and inactive Ω_I do not contribute to the Hamiltonian.

The two-phases and three-phase coexistence as well as phase transitions between ordered lamellar phase, disordered structured phase and disordered structure-less phases were previously described by this model when amphiphiles are always active and the respective phase diagram was derived within the mean field approach [36]. We next investigate numerically the effects of intermittent dynamics of amphiphiles.

We use kinetic Monte-Carlo simulations to investigate the lattice model. The system evolves from a random initial configuration through the pair-swap dynamics of the two nearest neighbors randomly chosen (within 4-neighborhood). The swap is executed with probability 1 if the system’s energy difference ΔE calculated from the Hamiltonian Eq. (1) after the proposed swap is negative, and with probability $P_{\text{swap}} = \exp(-\Delta E/k_B T)$ otherwise. All interaction energies are normalized by $k_B T$, where k_B is the Boltzmann constant and T is the temperature. To be able to provide a fair comparison of an active and a passive system, in the passive counterpart, we introduce two amphiphile species (active and inactive) which are present in fixed proportions ($k_{\text{on}}/(k_{\text{on}} + k_{\text{off}})$

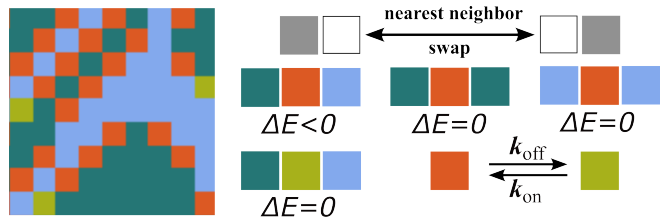


FIG. 1: Schematic representation of the lattice model of a microemulsion, each lattice site is occupied by any one of the components A (teal), B (blue) and two types of amphiphiles active Ω (orange) and inactive Ω_I (olive). Simulation dynamics involves randomly chosen two distinct nearest-neighbor pair-swap considering four nearest neighbors of any site. Ω reduces system energy by sitting between A and B , ΔE denotes the difference in energy after a swap. Intermittency of amphiphiles is introduced by switching Ω to Ω_I with rate k_{off} and the reverse with rate k_{on} .

and $k_{\text{off}}/(k_{\text{on}} + k_{\text{off}})$ respectively) and never switch their identities.

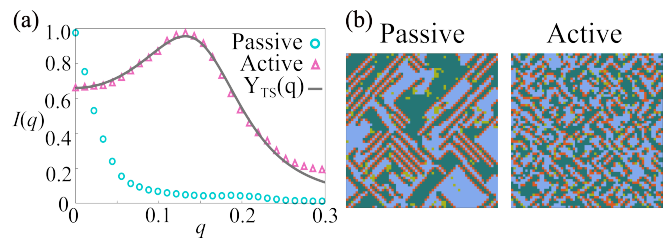


FIG. 2: Density fluctuations in the lattice configuration images are quantified by static structure factor in Fourier domain. (a) Radial intensity distribution in Fourier domain of lattice configuration in passive and active systems is shown. Unlike the disordered unstructured phase in the passive case (blue circles), the disordered structured or microemulsion phase in the active case (magenta triangles) has a peak at the absolute value of the wave vector $q > 0$. The form of the intensity distribution in the active case is compared with the phenomenological Landau theory of scattering intensity distribution of a microemulsion ($Y_{TS}(q)$) which shows a q^{-4} decay for large q values (see text). (b) Lattice configurations of passive and active cases with parameters mentioned in the text display how activity in the form of intermittent dynamics transforms the structure of the disordered phase.

To characterize the organization of microemulsion we measured the static structure factor which is defined as the Fourier transform of the density-density correlation function of any of the components A, B and Ω . In simulations, we collect the images of the steady-state configurations (after a prolonged equilibration phase) of a particular phase characterized by fixed parameters of density ratios, interactions, and turnover rates. Specifically, the structure factor is defined as $I(q) = \langle \rho_A(q) \rho_A(-q) \rangle_q$ [37]. Here, $\rho_A(q)$ is the Fourier transform of the im-

age intensity and $q = |\mathbf{q}| = \sqrt{q_x^2 + q_y^2}$ is the absolute value of the wave vector. In Fig.2a, we show $I(q)$ obtained for particle densities $A = B = 0.35$ and $\Omega = 0.30$, particle interactions $J_{AA} = J_{BB} = 2.5$, $J_{AB} = 0$ and $J_\Omega = 3.0$ and intermittent rates $k_{\text{on}} = 0.90$, $k_{\text{off}} = 0.10$, and $L = 64$. For the selected parameters, we see that a passive system corresponds to a disordered unstructured phase as the structure factor has no peak; see open circles in Fig.2a and the snapshot of respective simulations in Fig.2b left panel. Remarkably, the same composition with amphiphile turnover is a disordered structured phase or a microemulsion phase, as seen by the occurrence of a distinct peak in the structure factor, shown by open triangles in Fig.2a and illustrated by the snapshot in Fig.2b, right panel. Interestingly, we can use the expression of the structure factor $Y_{TS}(q)$ derived from a phenomenological equilibrium microemulsion theory [38] as a fitting function for the case of active microemulsion: $Y_{TS}(q) \sim (a + c_1 q^2 + c_2 q^4)^{-1}$, which with negative c_1 first reaches a maximum before it decays as q^{-4} .

Thus, we see that the activity of amphiphiles can change the structural organisation of the microemulsion. We also notice that the dynamics of two systems (see Supplemental Movies 1 and 2) is also distinctly different. To get a better insight into dynamics, we can take advantage of the lattice model that allows for coarse-graining and the derivation of a continuum theory.

Coarse grained continuum theory.- Considering the nearest neighbour interactions we coarse grain the system to derive the continuum description for the free energy density as discussed in Supplemental Material [39]:

$$\begin{aligned} \mathcal{F} = & -\frac{J_{AA}}{2} \left(A^2 - \frac{1}{2} (\nabla A)^2 \right) - \frac{J_{BB}}{2} \left(B^2 - \frac{1}{2} (\nabla B)^2 \right) \\ & - J_\Omega \left(\Omega (2AB - 4\nabla A \cdot \nabla B) \right) - \Omega (A^2 + B^2 - 2(\nabla A)^2 \\ & - 2(\nabla B)^2) + A \ln A + B \ln B + \Omega \ln \Omega + \Omega_I \ln \Omega_I, \quad (2) \end{aligned}$$

where A , B and Ω denote the densities of the corresponding components (and $\Omega_I = 1 - A - B - \Omega$). Next, we can derive the dynamical equations for different phases. The particle number conservation of A , B and Ω can be expressed by the continuity equations. In the linear response regime, the particle current is proportional to the thermodynamic force of the gradient of the chemical potential and thus can be written in terms of the free energy functional:

$$\partial_t A = \Gamma_A \nabla \cdot \left(\nabla \frac{\delta \mathcal{F}}{\delta A} \right), \quad \partial_t B = \Gamma_B \nabla \cdot \left(\nabla \frac{\delta \mathcal{F}}{\delta B} \right), \quad (3)$$

$$\partial_t \Omega = \Gamma_\Omega \nabla \cdot \left(\nabla \frac{\delta \mathcal{F}}{\delta \Omega} \right) + k_{\text{on}} \Omega_I - k_{\text{off}} \Omega, \quad (4)$$

where $\Gamma_{A,B,\Omega}$ is the diffusion coefficient for particles at unit temperature. For constant temperature, and assuming that all particles are moving through nearest neighbor swap at the same rate, the diffusion coefficients for

all types of particles are considered to be the same. The nonequilibrium contribution of the amphiphile turnover is in the chemical reaction turnover terms in the last equation, which is not derived as a part of the free-energy current. We now perform numerical simulations of this continuum model and show that it qualitatively reproduces the phase separation patterns as previously observed in the lattice simulations (see Fig. 3a), where parameters are such that the passive system is in the lamellar state, and its active counterpart is in the microemulsion state. We next aim to calculate the intermediate scattering function (ISF) [40] to quantify the relaxation dynamics in our system.

To simplify calculations further, we introduce a change of variables by two modified local densities $\Phi = A + B$ and $\Psi = A - B$ which will enable us to perform a linear stability analysis. We further assume that density of A and B phases are equal as well as the pair interactions of similar kind of particles ($J_{AA} = J_{BB}$). The diffusion coefficient for the modified local densities turn out to be $\Gamma_{\Phi,\Psi} = \Gamma_A + \Gamma_B$. Thus obtained dynamical equations are then used to deduce the ISF as the solutions of these equations in the Fourier domain as discussed in Supplemental Material [39]. For the density component Φ , the ISF is given by,

$$F_\Phi(q, \tau) = S_\Phi(q) e^{\tau \beta_\Phi(q)}, \quad (5)$$

where $S_\Phi(q)$ is defined as the static structure factor which can be obtained from the initial condition and can also be denoted as $F_\Phi(q, 0)$ and τ is the time interval. In Fig.3b, we plot $F_\Phi(q, \tau)/F_\Phi(q, 0)$, which according to Eq. (5) is an exponential function and compare it to the simulation results of the lattice model at a particular value of q where the radial distribution has a maximum. We see that the theoretical prediction holds for two orders of magnitude in time before the simulated correlations rapidly decrease. Importantly, active amphiphile turnover does not affect this relaxation dynamics.

The situation is markedly different for the amphiphile component Ω . The solution is more involved, as it contains terms stemming from the non-conserved reaction flux because of intermittent dynamics. With a little algebra as shown in Supplemental Material [39], its ISF reads:

$$\begin{aligned} F_\Omega(q, \tau) = & \left(S_\Omega(q) + k_{\text{on}} - \frac{S_{\Phi\Omega}(q)\zeta(q)}{\beta_\Phi(q) - \beta_\Omega(q)} \right) e^{\tau \beta_\Omega(q)} \\ & + \left(\frac{S_{\Phi\Omega}(q)\zeta(q)}{\beta_\Phi(q) - \beta_\Omega(q)} \right) e^{\tau \beta_\Phi(q)} \quad (6) \end{aligned}$$

Eq. (6) contains the static structure factor $S_\Omega(q)$ which involves a single density component and $S_{\Phi\Omega}(q)$ coupling both density components as well as terms $\beta_\Phi(q)$, $\beta_\Omega(q)$, k_{on} , k_{off} and $\zeta(q, k_{\text{on}})$ as discussed in Supplemental Material [39]. We have no direct analytical method

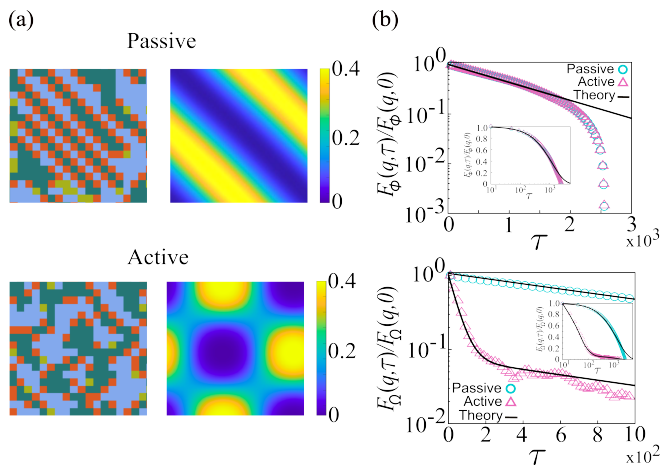


FIG. 3: (a) Both lattice configuration from simulation as well as density map from coarse-grained theory show lamellar-like structure in the passive case whereas microphase separated structure appears in the active case. The simulation and the coarse-grained density map are obtained with the same parameters as in Fig.2. The simulation figure is the same as Fig.2b with zoomed in regions to show the structure clearly. (b) Relaxation dynamics in terms of ISF performed at a particular value of q where the radial distribution has a maximum ($q = \sqrt{q_x^2 + q_y^2}$, $q_x = q_y = 1/L$), for each density component Φ and Ω . They behave similarly in the passive case, but qualitatively different in terms of fast decay as a superposition of two exponentials for Ω in the active case. Here, points are from simulations and solid lines are from the coarse-grained theory. Inset shows the same plot in the log-linear scale. Time scale is in Monte Carlo steps and the parameters of the continuum theory are adjusted to match this time.

to calculate $S_{\Omega}(q)$ and $S_{\Phi\Omega}(q)$, so we use them as fit parameters when comparing with the simulation results. We have also determined these values numerically in the lattice simulations and found that $S_{\Phi\Omega}(q)$ has a negative sign, which indicates that the two density components are anti-correlated. $F_{\Omega}(q, \tau)$ is a superposition of two exponentials as revealed in Fig.3b. For Ω , the active system shows an additional fast relaxation time dependent on the amphiphile turnover $\beta_{\Omega}(q, k_{\text{on}}, k_{\text{off}})^{-1}$ and then crosses over to a slower relaxation dynamics common to all components of the system which is independent of turnover $\beta_{\Phi}(q)^{-1}$. Lastly, we asked what other signatures of non-equilibrium we could identify by observing the dynamics of the system.

Local entropy production.- Entropy production is a key concept in nonequilibrium statistical physics, quantifying time-reversal symmetry breaking and thus represents a measure of irreversible changes occurring within the system. Here, we use an information-theoretic approach to quantify the entropy production through the methodology, rooted in the context of compression algorithms.

By introducing non-conservative reaction flux arising from intermittent dynamics within the active system, our

focus is now to delineate the regions of entropy production as a direct manifestation of the nonequilibrium signature. Entropy production can be measured in terms of Kullback-Leibler divergence [41], which quantifies the difference between two probability distributions associated with time-forward and time-reversed system's trajectories. Consequently, it is a positive dimensionless value that signals system's departure from equilibrium. The method of measuring local entropy production is based on the concept of cross-parsing complexity [42, 43] and was formulated as an optimized estimator from the time series of system's dynamics [44]. Following recent work [45] that provides an example of applying it on a two-dimensional system of active Brownian particles, we use this model-free method to extract entropy production from the dynamics of our active microemulsion model (see [39] for technical details).

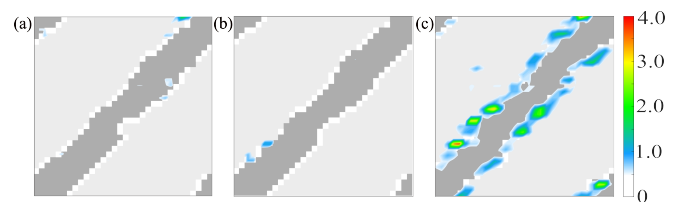


FIG. 4: Local entropy production-map (shown in color) for the microemulsion state in passive case (a), in case of active intermittent amphiphiles within thermal equilibrium (b) and for active intermittent amphiphiles in nonequilibrium (c). A - B interface here (initial snapshot of the system is shown in greyscale) is generated with a proper choice of lattice model parameters for each case. Entropy production is obtained by quantifying the occurrence of time reversal symmetry breaking events (see Supplemental Material [39]). High levels of entropy production are detected at the A - B interface for the active case, whereas no entropy production is present for the other two cases.

To this aim we start with densities $A = 0.67$, $B = 0.26$ and aforementioned interactions and intermittent rates, such that a clear and stable A - B interface (lamellar phase) is observed in the steady state both for the passive and active systems. Furthermore, we explore a third model variant in which amphiphile turnover is allowed, albeit under conditions of thermal equilibrium, as discussed in the Supplemental Material [39]. We notice that the A -rich and B -rich regions have practically no change of configuration, as they are energetically stable. Mostly, the changes occur at the A - B interface. For the passive case this interface is also stable, recording no entropy production as indicated with color scale overlaid on top of initial system's configuration (shown in grey scale) Fig.4a. In situations involving amphiphile turnover under thermal equilibrium, the scenario is very similar (see Fig.4b). However, for the nonequilibrium case we observe a clear entropy production at the interface (see Fig.4c) signifying time-irreversible particle interchanges.

In conclusion, we have shown that the active turnover of amphiphiles in a microemulsion system changes both its structure and its dynamics. Starting with a classical lattice model, we also studied its coarse-grained counterpart and investigated its relaxation dynamics. Activity of the amphiphile turnover manifests itself in an additional relaxation time scale emerging in the intermediate structure factor function associated with the amphiphile. Consistent with those observations, local entropy production occurs at the interface between the phase separating components. This developed approach thus can also be used in the experimental systems of chromatin organisation. Fluorescent labeling of DNA would provide access to structural information [46] while fluorescently labeled polymerase molecules will allow to quantify relaxation dynamics and link signatures of nonequilibrium behavior to transcriptional activity. This work therefore lays grounds for the description of active microphase separated systems as they now recognized across multiple biological processes and active systems.

-
- [1] P. Sartoria and S. Leibler, PNAS **117**, 114–120 (2020).
- [2] A. I. Curatolo, N. Zhou, Y. Zhao, C. Liu, A. Daerr, J. Tailleur, J.-D. Huang, Nature Physics **16**, 1152–1157 (2020).
- [3] U. Marini, B. Marconi and C. Maggi, Soft Matter, **11**, 8768–8781 (2015).
- [4] É. Fodor, C. Nardini, M. E. Cates, J. Tailleur, P. Visco, and F. van Wijland, Phys. Rev. Lett. **117**, 038103 (2016).
- [5] S. Ramaswamy, Annu. Rev. Condens. Matter Phys. **1**, 323–345 (2010).
- [6] H. Su, C.-A. Hurd Price, L. Jing, Q. Tian, J. Liu, and K. Qian, Materials Today Bio **4** p. 100033 (2019).
- [7] J. Katuri, X. Ma, M. M. Stanton, and S. Sánchez, Accounts of chemical research **4** pp. 2–11 (2017).
- [8] A. Fritsch, A. F. Diaz-Delgado, O. Adame-Arana, C. Hoegge, M. Mittasch, M. Kreysing, M. Leaver, A. Hyman, F. Jülicher, C. A. Weber, Proc. Natl. Acad. Sci U.S.A., **118**, 37 (2021).
- [9] J. Prost, F. Jülicher and J. F. Joanny, Nat. Phys. **11**, 111–7 (2015).
- [10] M.K. Transtrum, P. Qiu, PLoS Comp. Biol. **12**, e1004915 (2016).
- [11] H-S. Kuan, W. Pönisch, F. Jülicher and V. Zaburdaev, Phys. Rev. Lett. **126**, 018102 (2021).
- [12] J. Toner, Y. Tu, S. Ramaswamy, Ann. of Physics, **318**, 170–244 (2005).
- [13] M. C. Marchetti, J. F. Joanny, S. Ramaswamy, T. B. Liverpool, J. Prost, M. Rao, and R. A. Simha, Rev. Mod. Phys. **85**, 1143 (2013).
- [14] J. F. Joanny and J. Prost HFSP Journal **3**, 94–104, (2009).
- [15] A. A. Hyman, C. A. Weber and F. Jülicher, Annu. Rev. Cell Dev. Biol. **30** 39–58, (2014).
- [16] A. Ianiro, H. Wu, M. M. J. van Rijt, M. P. Vena, A. D. A. Keizer, A. C. C. Esteves, R. Tuinier, H. Friedrich, N. A. J. M. Sommerdijk and J. P. Patterson, Nature Chemistry **11** 320–328, (2019).
- [17] C. A. Weber, D. Zwicker, F. Jülicher and C. F. Lee, Rep. Prog. Phys. **82**, 064601 (2019).
- [18] L. Hilbert Y. Sato, K. Kuznetsova, T. Bianucci, H. Kimura, F. Jülicher, A. Honigmann, V. Zaburdaev and N. L. Vastenhouw, Nature Communications **12**, 1360 (2021).
- [19] B.M. Knickerbocker, C.V. Pesheck, H.T. Davis, and L.E. Scriven, J. Phys. Chem. **86**, 393 (1982).
- [20] M. Kahlweit, R. Strey, P. Firman, and D. Haase, Langmuir **1**, 281 (1985).
- [21] J. C. Wheeler and B. Widom, J. Am. Chem. Soc. **90**, 3064, (1968).
- [22] S. A. Safran and L. A. Turkevich, Phys. Rev. Lett. **50**, 1930 (1983).
- [23] B. Widom, J. Chem. Phys. **81**, 1030 (1984).
- [24] S. A. Safran, D. Roux, M. E. Cates, and D. Andelman, Phys. Rev. Lett. **57**, 491 (1986).
- [25] D. Andelman, M. E. Cates, D. Roux, S. A. Safran, J. Chem. Phys. **87**, 7229, (1987).
- [26] B. Widom, J. Phys. Chem. **88**, 6508 (1984).
- [27] R. G. Larson, L. E. Scriven, H. T. Davis, J. Chem. Phys. **83**, 2411 (1985).
- [28] B. Widom, J. Chem. Phys. **84**, 6943 (1986).
- [29] K. Chen, C. Ebner, C. Jayaprakash, and R. Pandit, Phys. Rev. A **38**, 6240 (1988).
- [30] R. G. Larson, J. Chem. Phys. **96**, 7904 (1992).
- [31] G. Gompper and M. Schick, Phys. Rev. Lett. **62**, 1647 (1989).
- [32] N. Schneider, F.-G. Wieland, D. Kong, A. A. M. Fischer, M. Hörner, J. Timmer, H. Ye and W. Weber, Sci. Adv. **7**, eabd3568 (2021).
- [33] K. Wagh, D. A. Garcia, A. Upadhyaya, Current Opinion in Structural Biology, **71**, 148–155 (2021).
- [34] B. Wang, L. Zhang, T. Dai, Z. Qin, H. Lu, L. Zhang and F. Zhou, Signal Transduction and Targeted Therapy, **6**, 290 (2021).
- [35] G. Gompper and M. Schick, Phys. Rev. B **41**, 9148 (1990).
- [36] G. Gompper and M. Schick, Phys. Rev. A **42**, 2137 (1990).
- [37] J.-P. Hansen and I. R. McDonald, Theory of Simple Liquids (Academic, London, 1986).
- [38] M. Teubner and R. Strey, J. Chem. Phys. **87**, 3195–3200 (1987).
- [39] See Supplemental Material for further details.
- [40] C. Kurzthaler, S. Leitmann and T. Franosch, Sci. Rep. **6**, 36702 (2016).
- [41] S. Kullback, R. A. Leibler, Ann. Math. Statist. **22**, 79–86 (1951).
- [42] J. Ziv and N. Merhav, IEEE Trans. Inf. Theory **39**, 1270 (1993).
- [43] A. D. Wyner, J. Ziv, and A. J. Wyner, IEEE Trans. Inf. Theory **44**, 2045 (1998).
- [44] É. Roldán and Juan M. R. Parrondo, Phys. Rev. E **85**, 031129 (2012).
- [45] S. Ro, B. Guo, A. Shih, T. V. Phan, R. H. Austin, D. Levine, P. M. Chaikin and S. Martiniani, Phys. Rev. Lett. **129**, 220601 (2022).
- [46] A. Noa, H.S. Kuan, V. Aschmann, V. Zaburdaev, and L. Hilbert, PLOS Comp. Bio. **17**(5): e1008974 (2021).

Supplementary Material for “Non-equilibrium structure and relaxation in active microemulsions”

A. Coarse-grained representation

We start from the microscopic description of the Hamiltonian in terms of the occupancy operator to frame the continuum model via coarse-graining for the microemulsion system in equilibrium. In terms of the occupancy operator $\eta_i^{A,B,\Omega,\Omega_I}$ which becomes unity if the site i is occupied by the respective component and zero otherwise, is given by Eq. (1) in main text. Now, when we introduce the intermittent dynamics $\eta_i^\Omega \xrightarrow{k_{\text{off}}} \eta_i^{\Omega_I}$, $\eta_i^{\Omega_I} \xrightarrow{k_{\text{on}}} \eta_i^\Omega$ are not coupled with system energy, Ω 's and Ω_I 's do not appear in the Hamiltonian. They enter later at the dynamical equations. On the other hand, when the intermittent dynamics are in accordance with the system energy, we can write the free energy expression considering the intermittent rates in terms of chemical potential as discussed in sec. D.

Now, by considering the nearest neighbour interactions where the amphiphile-mediated interaction involves three components in a line, we can use the criteria $A_i A_{i+1} = (A_i^2 + A_{i+1}^2 - (A_{i+1} - A_i)^2)/2$ and $A_i B_{i+1} = (A_i B_i + A_{i+1} B_{i+1} + A_i(B_{i+1} - B_i) - (A_{i+1} - A_i)B_{i+1})/2$, then the Hamiltonian can be written as,

$$\begin{aligned} \mathcal{H} = & \frac{1}{2} \sum -J_{AA} \frac{A_i^2 + A_{i+1}^2 - (A_{i+1} - A_i)^2}{2} - J_{BB} \frac{B_i^2 + B_{i+1}^2 - (B_{i+1} - B_i)^2}{2} \\ & - J_\Omega \Omega_{i+1} \left(A_i B_i + A_{i+2} B_{i+2} + (A_{i+2} - A_i)(B_{i+2} - B_i) \right. \\ & \left. - \frac{A_i^2 + A_{i+2}^2 - (A_{i+2} - A_i)^2}{2} - \frac{B_i^2 + B_{i+2}^2 - (B_{i+2} - B_i)^2}{2} \right) \end{aligned} \quad (\text{S1})$$

In the mean-field approximation, $A_i = A + \delta s_i$, where $A = \langle A_i \rangle$, δs_i is the corresponding fluctuation and $\langle \dots \rangle$ denotes ensemble average. So, the coarse-grained values of A_i, B_i, Ω_i can be understood as the averages of their microscopic quantities at the position i . The coarse-grained Hamiltonian then reads:

$$\begin{aligned} \mathcal{H} = & -\frac{J_{AA}}{2} \left(A^2 - \frac{1}{2} (\nabla A)^2 \right) - \frac{J_{BB}}{2} \left(B^2 - \frac{1}{2} (\nabla B)^2 \right) \\ & - J_\Omega \Omega \left(2AB - 4\nabla A \cdot \nabla B - (A^2 + B^2 - 2(\nabla A)^2 - 2(\nabla B)^2) \right) \end{aligned} \quad (\text{S2})$$

The corresponding free energy density is shown by Eq. (2) in the main text, here we have considered the same order of expansion for all the components, *i.e.* up to two lattice spacing.

Eq. (2) in the main text consists of the interaction energy terms as well as the terms due to free energy of mixing. The free energy of mixing is a concept in thermodynamics that describes the increase in entropy when two or more different substances are mixed together. The mixing always increases the entropy of the system, consistent with the second law of thermodynamics. It is worth noting that the expression assumes an ideal mixing scenario, where the interactions between different components are negligible compared to the thermal energy of the system. In more complex scenarios, such as non-ideal solutions or mixtures with significant inter-particle interactions, additional terms may need to be included in the free energy expression. The entropy of random mixing is written as a function of the volume fraction of each components as shown by Eq. (2) in main text. Here, we have only considered interaction between similar components e.g. J_{AA} and J_{BB} , and $J_{AB} = 0$.

Now, we formulate the dynamics that governs the microphase separation. The equations that incorporate density components A and B are applicable in both equilibrium and non-equilibrium conditions. However, the equation that includes Ω is exclusively pertinent to nonequilibrium conditions due to its association with intermittent dynamics not coupled to thermodynamic equilibrium. Conservation of components A, B, Ω and Ω_I can be represented by the continuity equations. In the linear response regime, the dynamical equations are given by Eq. (3-4) in the main text.

For each component in the system they can be written explicitly as,

$$\begin{aligned}
\partial_t A &= \Gamma_A \nabla \cdot \nabla \left(-J_{AA} \left(A + \frac{\nabla^2 A}{2} \right) - J_\Omega \left(2\Omega B + 4\Omega \nabla^2 B - 2\Omega A - 4\Omega \nabla^2 A \right) + \ln A - \ln(1 - A - B - \Omega) \right) \\
\partial_t B &= \Gamma_B \nabla \cdot \nabla \left(-J_{BB} \left(B + \frac{\nabla^2 B}{2} \right) - J_\Omega \left(2\Omega A + 4\Omega \nabla^2 A - 2\Omega B - 4\Omega \nabla^2 B \right) + \ln B - \ln(1 - A - B - \Omega) \right) \\
\partial_t \Omega &= \Gamma_\Omega \nabla \cdot \nabla \left(-J_\Omega \left(2AB + 4\nabla A \cdot \nabla B - A^2 - B^2 + 2(\nabla A)^2 + 2(\nabla B)^2 \right) + \ln \Omega - \ln(1 - A - B - \Omega) \right) \\
&\quad - k_{\text{off}} \Omega + k_{\text{on}} (1 - A - B - \Omega)
\end{aligned} \tag{S3}$$

For the sake of simplifying the equations, we have introduced two modified local densities $\Phi = A + B$ and $\Psi = A - B$. The dynamical equations with the modified local densities can be written as:

$$\begin{aligned}
\partial_t \Phi &= \Gamma_\Phi \nabla \cdot \nabla \left(-\frac{J_{AA}}{2} (\Phi + \nabla^2 \Phi) + \frac{J_{AA}}{4} \nabla^4 \Phi + \frac{1}{2} \ln \frac{\Phi + \Psi}{2} + \frac{1}{2} \ln \frac{\Phi - \Psi}{2} - \ln(1 - \Phi) \right) \\
\partial_t \Omega &= \Gamma_\Omega \nabla \cdot \nabla \left(-J_\Omega \left(-\Psi^2 + 2(\nabla \Psi)^2 \right) + \ln \Omega - \ln(1 - \Phi - \Omega) \right) - k_{\text{off}} \Omega + k_{\text{on}} (1 - \Phi - \Omega)
\end{aligned} \tag{S4}$$

Here, the diffusion coefficient, represented by $\Gamma_{A,B,\Omega}$, corresponds to the movement of particles at unit temperature. If the temperature is held constant and it is assumed that all particles are transitioning through nearest neighbor exchange at an equivalent rate, then the diffusion coefficients for all particle varieties are deemed identical. The diffusion coefficient for the modified local densities turn out to be $\Gamma_{\Phi,\Psi} = \Gamma_A + \Gamma_B$.

We next take the two density components Φ and Ω to investigate the relaxation dynamics. For this, we need to derive the time evolution of the density-density correlation, *i.e.* the Intermediate Scattering Function (ISF). As cross-correlation functions are easier to analyse in Fourier domain, we do so for the rest of the derivation.

We start with a small perturbation from the steady state Φ_0 and Ω_0 by setting $\Phi = \Phi_0 + \tilde{\Phi}$ and $\Omega = \Omega_0 + \tilde{\Omega}$. Here $\tilde{\Phi}$ and $\tilde{\Omega}$ denote small fluctuations. Using linear stability analysis in Fourier domain, Eq. (S4) becomes:

$$\begin{aligned}
\partial_t \tilde{\Phi} &= \Gamma_\Phi \left(-\left(\frac{1}{\Phi_0(1 - \Phi_0)} \right) q^2 + \frac{J_{AA}}{2} (q^2 - q^4) - \frac{J_{AA}}{4} q^6 \right) \tilde{\Phi} \\
\partial_t \tilde{\Omega} &= -\Gamma_\Omega \left(\frac{1}{\Omega_0} + \frac{1}{1 - \Phi_0 - \Omega_0} \right) q^2 \tilde{\Omega} - \Gamma_\Omega \left(\frac{1}{1 - \Phi_0 - \Omega_0} \right) q^2 \tilde{\Phi} - k_{\text{off}} \tilde{\Omega} + k_{\text{on}} (1 - \tilde{\Phi} - \tilde{\Omega})
\end{aligned} \tag{S5}$$

Eq. (S5) can be rewritten in a compact form as,

$$\partial_t \tilde{\Phi} = \beta_\Phi(q) \tilde{\Phi} \tag{S6}$$

$$\partial_t \tilde{\Omega} = \beta_\Omega(q) \tilde{\Omega} + \zeta(q) \tilde{\Phi} + k_{\text{on}} \tag{S7}$$

where we have defined

$$\begin{aligned}
\beta_\Phi(q) &= \Gamma_\Phi \frac{J_{AA}}{2} (q^2 - q^4) - \Gamma_\Phi \frac{J_{AA}}{4} q^6 - \Gamma_\Phi \left(\frac{1}{\Phi_0(1 - \Phi_0)} \right) q^2, \\
\beta_\Omega(q) &= -\Gamma_\Omega \left(\frac{1}{\Omega_0} + \frac{1}{1 - \Phi_0 - \Omega_0} \right) q^2 - k_{\text{on}} - k_{\text{off}}, \\
\zeta(q) &= -\Gamma_\Omega \left(\frac{q^2}{1 - \Phi_0 - \Omega_0} \right) - k_{\text{on}}.
\end{aligned}$$

B. Intermediate scattering function

In the realm of statistical physics, particularly in the study of systems undergoing dynamic processes, the intermediate scattering function serves as a fundamental quantity. It plays a pivotal role in characterizing the temporal

evolution of correlation functions in these systems. The ISF is primarily utilized in the context of dynamic structure factor, which describe the spatial and temporal correlations of fluctuations in a system's density or other relevant order parameters. Specifically, the ISF quantifies how these correlations evolve over time. Technically, the intermediate scattering function $F(q, t)$ is defined as the time correlation function of the fluctuations in the scattered intensity at a given wave vector q .

In simulations, the ISF is obtained by measuring the time-dependent structure factor, which captures the spatial correlations of fluctuations at different times. By analyzing the decay of the ISF over time, one can extract crucial information about the dynamic behavior of the system, including the presence of relaxation processes and the nature of collective phenomena such as diffusion, it also sheds light on the dynamic behavior of matter at various length and time scales.

As we already have the dynamical equations in the Fourier space given by Eq. (S6) and Eq. (S7), we can proceed to get the ISF from there. The solution for Eq. (S6) is simple and given by Eq. (5) in the main text. The dynamical structure factor can be obtained by the Laplace transformation of Eq. (S6) and Eq. (S7). The Laplace transform of the time derivative in general yields $\mathcal{L}(f'(t)) = \omega f(\omega) - f(0)$. Thus from Eq. (S6) and Eq. (S7) we get,

$$\begin{aligned} w\tilde{\Phi} - \tilde{\Phi}(0) &= \Gamma_{\Phi} \left(- \left(\frac{1}{\Phi_0(1-\Phi_0)} \right) q^2 \tilde{\Phi} + \frac{J_{AA}}{2} (q^2 - q^4) \tilde{\Phi} - \frac{J_{AA}}{4} q^6 \tilde{\Phi} \right) \\ &= \beta_{\Phi}(q) \tilde{\Phi} \end{aligned} \quad (\text{S8})$$

$$\begin{aligned} w\tilde{\Omega} - \tilde{\Omega}(0) &= \Gamma_{\Omega} \left(- \left(\frac{1}{\Omega_0} + \frac{1}{1-\Phi_0-\Omega_0} \right) q^2 \tilde{\Omega} - \left(\frac{1}{1-\Phi_0-\Omega_0} \right) q^2 \tilde{\Phi} \right) - k_{\text{off}} \tilde{\Omega} + k_{\text{on}} (1 - \tilde{\Phi} - \tilde{\Omega}) \\ &= \beta_{\Omega}(q) \tilde{\Omega} + \zeta(q) \tilde{\Phi} + k_{\text{on}} \end{aligned} \quad (\text{S9})$$

The dynamical structure factor from Eq. (S8) and Eq. (S9) can be written as,

$$S_{\Phi}(q, w) = \frac{S_{\Phi}(q)}{w - \beta_{\Phi}(q)} \quad (\text{S10})$$

$$S_{\Omega}(q, w) = \frac{S_{\Omega}(q)}{w - \beta_{\Omega}(q)} + \frac{\zeta(q) S_{\Phi\Omega}(q)}{(w - \beta_{\Phi}(q))(w - \beta_{\Omega}(q))} + \frac{k_{\text{on}}}{w - \beta_{\Omega}(q)} \quad (\text{S11})$$

where $S_{\Phi}(q)$ and $S_{\Omega}(q)$ are the static structure factor for the respective density components Φ and Ω respectively. $S_{\Phi\Omega}(q)$ is the coupled static structure factor and $S_{\Phi\Omega}(q, w) = \frac{S_{\Phi\Omega}(q)}{w - \beta_{\Phi}(q)}$ is the coupled dynamical structure factor involving both density components Φ and Ω . These are defined mathematically as:

$$S_{\Phi}(q, w) = \int_0^{\infty} e^{w\tau} \Phi(q, 0) \Phi^*(q, \tau) d\tau \quad (\text{S12})$$

$$S_{\Phi\Omega}(q, w) = \int_0^{\infty} e^{w\tau} \Phi(q, 0) \Omega^*(q, \tau) d\tau \quad (\text{S13})$$

There is no direct method to calculate the static structure factors $S_{\Omega}(q)$ and $S_{\Phi\Omega}(q)$ through coarse-grained analytical treatment. To this end, we measured these values numerically and noticed that $S_{\Phi\Omega}(q)$ has negative sign, which indicates the two density components Φ and Ω are anti-correlated. We have assigned these terms as fitting parameters in the analytical expression to get the final solution and compare with the numerical result.

Now, the solution of the Eq. (S7) is not so straight-forward to find out the ISF. So, we adopted another way to deduce the ISF through inverse Laplace transformation of the dynamical structure factor from Eq. (S11). In this way we get the ISF for the density component Ω as shown by Eq. (6) in the main text.

To measure the relaxation in terms of the ISF numerically, we start with the time evolution of lattice configurations from a random initial state. We generate time evolution of lattice configuration images which consist of lattice sites occupied with either of the density component A , B or Ω only for which the relaxation is measured. For example, to measure the relaxation of A , each image only consists of sites with A and rest of the lattice space is empty. Similarly, to measure relaxation of $\Phi = A + B$, each image has sites only occupied with A and B . To suppress the noise, we measure the average occupancy of each lattice site considering all the time evolution configurations, and subtract it from every lattice site of each configuration. Then we transform each lattice configuration image in the Fourier domain through the two dimensional Fast Fourier Transform (FFT2).

In our simulations, ISF is obtained by measuring the density correlation of fluctuations at different times as,

$$F(q, \tau) = \frac{\sum_{t=1}^{M-\tau} \rho(q, t) \rho^*(q, t + \tau)}{M - \tau} \quad (\text{S14})$$

where $\rho(q, t)$ is the density map of an image at time t in Fourier domain, τ is the time interval over which the correlation is measured between two images and M steps are used for time averaging. For the q -value we chose the particular wave number in radial distribution of the images for which the intensity is maximum.

The density component Φ behaves identically for active and passive case and shows an exponential decay as given by Eq. (5) in the main text. Whereas the density component Ω behaves differently in terms of relaxation for passive and active cases. As in the active case it involves intermittent dynamics with two rates k_{on} and k_{off} as given by Eq. (6) in the main text. For active case it turns out to be a superposition of two exponential functions. This is why we observed the relaxation of $F_{\Omega}(q, \tau)$ as a rapid decay followed by a slower one.

C. Local entropy production

Local entropy production (\mathcal{E}_p) is a concept within the framework of irreversible thermodynamics that quantifies the rate at which entropy increases within a small region of a system. It provides valuable insights into the irreversible processes occurring at the microscopic level. \mathcal{E}_p focuses on analyzing entropy changes within small spatial regions of the system. To measure local \mathcal{E}_p , we track the system configurations for a given observation interval. The main idea is to observe the events of time reversal symmetry breaking (TSRB) at the interface of A and B components separated by Ω where the reversibility in lattice configuration is not preserved due to the system dynamics. We have measure the \mathcal{E}_p originating due to local microscale processes e.g. particle diffusion, energy transfer, or other irreversible interactions between neighboring lattice sites.

\mathcal{E}_p can be quantified by the Kullback-Leibler divergence which is defined as the difference between two probability distributions (PDF). Rather than measuring PDF of local configurations, it is a standard procedure to use the method based on the proposal first illustrated by Ziv and Merhav in terms of compression algorithms but without any association with the physical entropy. In this methodology, the system configurations in each time steps of a certain interval, are reduced to an array of numbers. They coined a quantity called cross parsing complexity \mathcal{C} which is defined as the sum of sequentially drawn longest arrays of numbers from one sequence while parsing through or iterates through all elements of another sequence. One sequence is derived from the randomly drawn system configuration, reduced into number of arrays for each forward time-step. The other sequence contemplates the time-span in reverse direction. Ziv and Merhav have defined \mathcal{C} as the difference between the cross parsing involving forward and reverse sequence, and the self incremental parsing of the forward sequence. Later, Roldán and Parrondo reported large error in the method adopted by Ziv and Merhav due to mixing of two types of parsing namely cross parsing and sequential self incremental parsing. So, the later work corrected the \mathcal{E}_p estimator by evaluating the cross parsing between different segments of the same trajectory and then subtracted that from the original Ziv and Merhav's estimator. We have used the \mathcal{E}_p estimator used by Roldán and Parrondo and followed the model free method for our lattice system to extract \mathcal{E}_p from system dynamics.

To do that, we start by overlaying a small grid of size 2×1 over the system and record the lattice configuration in each time-step. For a particular position of the grid, one can have a set of configurations corresponding to each time step in forward time-span. From this set we can get the quantity \mathcal{Z} by random sequentially drawn N number of configurations to form a forward sequence. Similarly, one can get a reverse sequence from the set created by having the configurations for each time step in the backward time-span denoted by \mathcal{Z}^* . Considering these two sequences, we can get the \mathcal{E}_p estimator proposed by Ziv and Merhav. Now, to evaluate the correction term Roldán and Parrondo divided the forward sequence into two equal parts, and measured the cross parsing between them. This term is subtracted from the original Ziv and Merhav's estimation to get the correct \mathcal{E}_p estimator, which can be written as:

$$\mathcal{E}_p = \lim_{N \rightarrow \infty} \frac{1}{N} \left(\mathcal{C}(\mathcal{Z} || \mathcal{Z}^*) \right) - \frac{1}{N/2} \left(\mathcal{C}(\mathcal{Z}_{N/2}^N || \mathcal{Z}_1^{N/2}) \right) \quad (\text{S15})$$

$$= \lim_{N \rightarrow \infty} \frac{1}{N} \left(\mathcal{C}(\mathcal{Z} || \mathcal{Z}^*) \ln N - \mathcal{C}(\mathcal{Z}) \ln \mathcal{C}(\mathcal{Z}) \right) - \frac{1}{N/2} \left(\mathcal{C}(\mathcal{Z}_{N/2}^N || \mathcal{Z}_1^{N/2}) \ln(N/2) - \mathcal{C}(\mathcal{Z}_{N/2}^N) \ln \mathcal{C}(\mathcal{Z}_{N/2}^N) \right) \quad (\text{S16})$$

The above equation consists of two cross-parsing complexities and specifically, the second term of Eq. (S15) represents the correction term proposed by Roldán and Parrondo. While in Eq. (S16) the second term from each

cross-parsing corresponds to the Shannon entropy of the constituent sequence. In Fig.4 of the main text, we have shown the entropy production-maps of the lattice system measured in this way for three different scenarios namely the passive case which is equilibrium and has no intermittent amphiphile dynamics, then the case with intermittent amphiphile dynamics but within chemical equilibrium, and, finally, the active case with intermittent amphiphile dynamics which drives the system out of equilibrium.

The main objective is to extract meaningful information or patterns from heterogeneous or diverse data sets that might be structured differently or follow varying conventions. It can be noticed from the entropy production-map that for passive case, the local \mathcal{E}_p is zero everywhere in the lattice. It could also be possible that they become very low approaching towards zero or only limited to positions where a few irreversible particle interchanges occur, which we attribute to numerical fluctuations. Intermittent dynamics within chemical equilibrium is showing also no \mathcal{E}_p . However, for the active case a high \mathcal{E}_p is observed throughout the interface. So, here we have shown that it is possible to identify the regions of the system that are driven out of equilibrium through this information-theoretic approach and this is also a promising tool to define such regions in experimental data.

It is also important to note that, we have introduced a scenario where the intermittent dynamics is consistent with chemical equilibrium to see whether the \mathcal{E}_p is mostly contributed from the intermittent dynamics itself or from the irreversible nonequilibrium type of dynamics. What we found is that, in the second case, though there are intermittent dynamics, but still no \mathcal{E}_p as the system is at equilibrium. Now we will discuss the case of intermittent dynamics within chemical equilibrium through mean-field analysis.

D. Dynamics within chemical equilibrium

We start with the system where the intermittent activity is within the thermodynamic equilibrium. The detailed balance condition for thermodynamic equilibrium is given by,

$$\Omega k_{\text{off}} = \Omega_I k_{\text{on}} \quad (\text{S17})$$

The free energy expression as Eq. (2) in the main text does not involve chemical reaction or intermittent dynamics. As molecular energy transformation is responsible for chemical reaction rates at the most fundamental level, chemical kinetics must provide some characteristics of molecular energies. So, a reversible chemical reaction involving active-inactive transition, gives rise to an additional term consisting of transition rates within the free energy density. Let's denote μ_Ω and μ_{Ω_I} as the chemical potentials of active and inactive amphiphiles respectively. The chemical potential represents the change in the free energy of the system when the number of particles of a particular species changes.

Now, the chemical potential of active and inactive amphiphiles can be written in terms of energy unit $k_B T$ as $\mu_\Omega = -\ln(\Omega N)$ and $\mu_{\Omega_I} = -\ln(\Omega_I N)$, where N is the total number of particles in the system, then ΩN and $\Omega_I N$ represents the total number of active and inactive amphiphiles respectively. As there is no empty space in the system, so $N = L \times L$. So, we can define the Free energy in thermodynamic equilibrium as,

$$\mathcal{F}' = \Omega N \mu_\Omega + \Omega_I N \mu_{\Omega_I} \quad (\text{S18})$$

So, adding this term with the free energy of interaction and mixing in the system, we get,

$$\begin{aligned} \mathcal{F}^{CEq} &= -\frac{J_{AA}}{2} \left(A^2 - \frac{1}{2} (\nabla A)^2 \right) - \frac{J_{BB}}{2} \left(B^2 - \frac{1}{2} (\nabla B)^2 \right) - J_\Omega \left(\Omega (2AB - 4\nabla A \cdot \nabla B) \right) \\ &\quad - \Omega (A^2 + B^2 - 2(\nabla A)^2 - 2(\nabla B)^2) + \left(A \ln A + B \ln B + \Omega \ln \Omega + (1 - A - B - \Omega) \ln(1 - A - B - \Omega) \right) \\ &\quad - \Omega N \ln(\Omega N) - (1 - A - B - \Omega) N \ln((1 - A - B - \Omega) N) \end{aligned} \quad (\text{S19})$$

It can be noticed that the last two terms of Eq. (S19) are in accordance with the intermittent dynamics within

thermodynamic equilibrium. Then the dynamical equation for Ω can be shown as,

$$\begin{aligned} \partial_t \Omega^{CEq} &= \Gamma_\Omega \nabla \cdot \nabla \left(-J_\Omega (2AB + 4\nabla A \cdot \nabla B - A^2 - B^2 + 2(\nabla A)^2 + 2(\nabla B)^2) \right. \\ &\quad \left. - (N-1) (\ln \Omega - \ln(1-A-B-\Omega)) \right) \end{aligned} \quad (\text{S20})$$

Adopting similar methodology with the modified local densities Φ and Ω and then applying small perturbation

from the steady state in the Fourier space, Eq. (S20) yields,

$$\partial_t \tilde{\Omega}^{CEq} = \Gamma_\Omega (N-1) \left(\frac{1}{\Omega_0} + \frac{1}{1-\Phi_0-\Omega_0} \right) q^2 \tilde{\Omega} + \Gamma_\Omega (N-1) \left(\frac{1}{1-\Phi_0-\Omega_0} \right) q^2 \tilde{\Phi} \quad (\text{S21})$$

Eq. (S21) can be written in a compact form as,

$$\partial_t \tilde{\Omega}^{CEq} = \beta_\Omega^{CEq}(q) \tilde{\Omega} + \beta_\Phi^{CEq}(q) \tilde{\Phi} \quad (\text{S22})$$

Where we have defined

$$\begin{aligned} \beta_\Omega^{CEq}(q) &= \Gamma_\Omega (N-1) \left(\frac{1}{\Omega_0} + \frac{1}{1-\Phi_0-\Omega_0} \right) q^2 \\ \beta_\Phi^{CEq}(q) &= \Gamma_\Omega (N-1) \left(\frac{1}{1-\Phi_0-\Omega_0} \right) q^2 \end{aligned}$$

Now, here we notice that the expression Eq. (S22) is independent of k_{on} and k_{off} , and in that sense it is different from the active system where the dynamical equation involving Ω depends on the intermittent rates that drives the system out of equilibrium.